NANO LETTERS

pubs.acs.org/NanoLett Letter

Thermally Switchable Nanogate Based on Polymer Phase Transition

Pauline J. Kolbeck,▽ Dihia Benaoudia,▽ Léa Chazot-Franguiadakis, Gwendoline Delecourt, Jérôme Mathé, Sha Li, Romeo Bonnet, Pascal Martin, Jan Lipfert, Anna Salvetti, Mordjane Boukhet, Véronique Bennevault, Jean-Christophe Lacroix, Philippe Guégan, and Fabien Montel*

Cite This: https://doi.org/10.1021/acs.nanolett.3c00438 Read Online

ACCESS | Metrics & More | Article Recommendations | Supporting Information

ABSTRACT: Mimicking and extending the gating properties of biological pores is of paramount interest for the fabrication of membranes that could be used in filtration or drug processing. Here, we build a selective and switchable nanopore for macromolecular cargo transport. Our approach exploits polymer graftings within artificial nanopores to control the translocation of biomolecules. To measure transport at the scale of individual biomolecules, we use fluorescence microscopy with a zero-mode waveguide set up. We show that grafting polymers that exhibit a lower critical solution temperature creates a toggle switch between an open and closed state of the nanopore depending on the temperature. We demonstrate tight control over the transport of DNA and viral capsids with a sharp transition (~1 °C) and present a simple physical model that predicts key features of this transition. Our approach provides the potential for controllable and responsive nanopores in a range of applications.

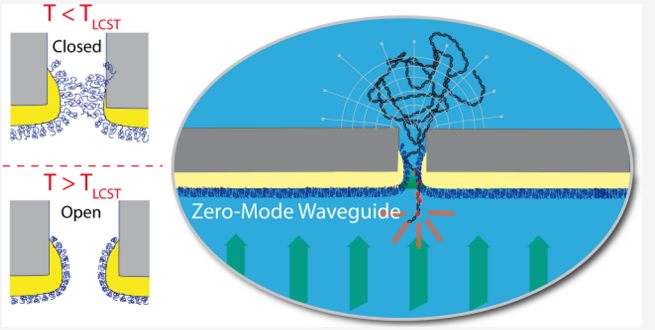

KEYWORDS: *nanopore, zero-mode waveguide, biomolecule filtration, thermoresponsive polymer, coil−globule transition*

The design of bioinspired nanopores brings the ability to manipulate and control ionic and molecular transport inside a confined environment and provides insight into ionic and molecular transport processes of biological channels.[1−6] Synthetic nanopores have many advantages over biological ones, such as their stability, tunable dimensions (size and shape), and the possibility of integration into nanofluidic systems.[7,8] By functionalizing the surface of the nanopore, their physical and chemical properties (e.g., hydrophobicity, selectivity, surface charges, and specific molecular recognition) and thus the ionic and molecular transport properties can be modified[2,9−15] and modeled using simulations.[16−18]

Poly(ethylene glycol) (PEG) polymer graftings have been employed previously to create a steric repulsive barrier that fills the interior of the nanopore.[3,4,19,20] The PEG grafting collapses by adding proteins in solution that bind to the network and induces a transition between poor and good solvent conditions. Poly(*N*-isopropylacrylamide) (PNIPAM) can also be used to coat the interior of the pore. PNIPAM is known for its hydrophobic−hydrophilic phase transition at physiological temperatures.[1,6,21] It has been previously shown that PNIPAM can be used to reproduce receptor-mediated transport in grafted nanopores.[1,21] More precisely, when grafted onto the pore surface and onto the transported molecule, it enables selective diffusive transport in an artificial system.

Nevertheless, none of these approaches has led to an efficient, reversible, and stable toggle switch that allows the transport of DNA and viral capsids through artificial membranes to be controlled in a temperature-modulated manner. In addition, transport in some of the previous studies was diffusive and molecular transport measurements were limited by aborted-diffusion events observed with electrical detection or accumulation effects due to adhesion on the membrane observed for simple fluorescence measurements.

To overcome these limitations, we built a thermally switchable nanopore as a gateway for the transport and filtration of DNA and viral capsids by electrografting temperature-responsive polymers on the nanopore membrane. We have used artificial polymers, poly(2-alkyl-2-oxazolines), as a new type of grafting inside the nanopore. Specifically, we used two types of poly(2-alkyl-2-oxazolines): hydrophilic poly(2-methyl-2-oxazoline) (PMeOx) and poly(2-*n*-propyl-2-oxazoline) (P*n*PrOx), which becomes hydrophobic at high temperature. For both polymers, we varied the molecular mass. The thickness of the grafted layer depends on both the type of polymer grafted and environmental conditions. PMeOx is in a good solvent at all temperatures around room temperature (20 °C) and can be considered an ideal coil. In contrast, P*n*PrOx

Received: February 3, 2023
Revised: May 16, 2023

https://doi.org/10.1021/acs.nanolett.3c00438
Nano Lett. XXXX, XXX, XXX−XXX

exhibits a lower critical solution temperature (LCST). Below the LCST this polymer is fully soluble in aqueous solution, whereas at temperatures higher than the LCST it aggregates and precipitates. This temperature dependence in a range compatible with biomolecules allows us to create a switch between an open and a closed state of the nanopore depending on the temperature inside the nanopore and thus create a switch for macromolecular transport inside through the nanopore. We demonstrate how the transport of biomolecules and viral capsids through artificial nanopores can be controlled by the type of grafted polymer inside the pore and switched on and off by an external stimulus.

Here, we used an optical approach, based on a zero-mode waveguide (ZMW) for nanopores,[19] to follow the transport of individual macromolecules in real time and at the scale of the single nanopore. To this end, the macromolecules were fluorescently labeled and driven through the nanopore by applying a pressure difference between the two sides of the membrane (Figure 1). A gold layer was vapor-deposited onto the membrane, onto which poly(2-alkyl-2-oxazolines) with different degrees of polymerization (X_n) were then electrografted, which either may or may not exhibit LCST (see Materials and Methods and sections S1, S2, and S9 in the Supporting Information for characterizations).

POLYMER GRAFTING INSIDE NANOPORE CREATES A THERMORESPONSIVE SWITCH FOR DNA TRANSLOCATION

With our ZMW for nanopores approach, we were able to directly observe individual DNA translocation events through polymer-grafted nanopores. We recorded and examined the translocation frequency for double-stranded DNA molecules (λ phage DNA) as a function of temperature for different polymer graftings inside the nanopore. The heating system we used controlled the temperature of the entire membrane (see Materials and Methods). The measurements were conducted for the P*n*PrOx and PMeOx graftings and for a membrane without polymer grafting as a negative control (Figure 2A and section S10 in the Supporting Information).

In the case of P*n*PrOx, we observed that the translocation frequency was strongly affected by temperature. A sharp drop in translocation frequency was observed when lowering the temperature in a narrow range around LCST. In contrast, for PMeOx grafted membranes, the translocation frequency remained unchanged with changes in temperature (Figure 2A). This behavior is consistent with the fact that P*n*PrOx possesses a LCST, such that a change in temperature in a range including the LCST switches the conformation of the polymers in the grafted layer between an extended and a collapsed phase. We interpret the changes in translocation frequency as a polymer toggle switch between an open (collapsed polymer) and a closed (extended polymer) state of the nanopore in response to the temperature of the surrounding medium (Figure 1).

To get quantitative results for the mean steepness of the transition m (in $°C^{-1}$) and the mean transition temperature θ (in °C), we fit the temperature−frequency curves for the P*n*PrOx grafting (Figure 2B and section S10 in the Supporting Information) by an error function $f(T)/f_{max} = 1/2\cdot(\mathrm{erf}(m\cdot(T-\theta)) + 1)$. The error bars were calculated as the standard errors. The steepness of the error function m is found to range between (0.58 ± 0.03 $°C^{-1}$ for $X_n = 33$ and 0.66 ± 0.05 $°C^{-1}$ for $X_n = 59$ (the complete set of values is shown in Table 1).

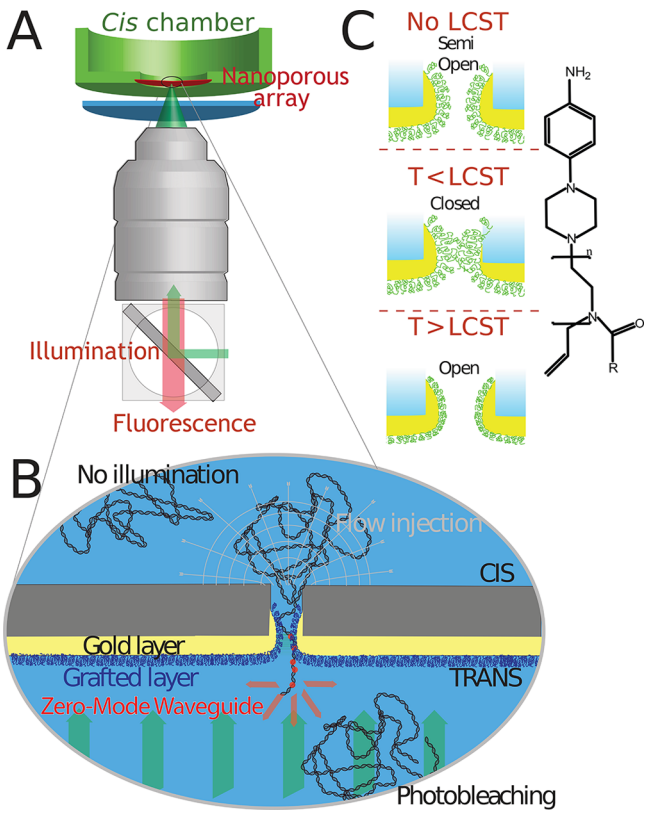

Figure 1. Zero-mode waveguide setup for nanopores with a grafted polymer. (A, B) Schematic of the zero-mode waveguide (ZMW) for nanopore setup. It uses a nanoporous array coated with a gold layer for near-field enhancement. When illuminated with a laser, the fluorescent molecules in the *cis* chamber do not receive any light because of the metal whereas downstream molecules are unfocused and bleached by the laser. Only the fluorescent molecules in the pore in the vicinity of the metal film are exposed to an enhancement of the electromagnetic field, which leads to reinforcement of the fluorescence. This methodology enables the detection of single-molecule translocation events with a high parallelization. In the case of nanoporous arrays functionalized with grafted polymers, the translocation of the transported molecule can be modulated by closing and opening the grafted channels. An examplary video recording of the translocation events can be found in section S12 in the Supporting Information. (C) Left: schematic of how grafted polymers modulate the pore diameter. Polymers that do not exhibit a lower critical solution temperature (LCST) limit the channel size but cannot completely close the pore. Pores grafted with polymers with an LCST can be triggered by changing the temperature to switch from an open state at high temperature to a closed state at low temperature. Right: Poly(2-alkyl-2-oxazoline) structure. The −R group corresponds to $-CH_3$ for PMeOx and to $-CH_2-CH_2-CH_3$ for PnPrOx.

This shows that the transition between the open state of the nanopore and the closed state is extremely sharp. A change in the surrounding temperature of less than 1 °C is already enough to evoke a conformational change of the polymer grafting and, with this, a change in the openness of the pore from a completely closed pore (no translocation events) to an open pore. The second fitting parameter is the midpoint position θ that gives the transition temperature. We find that this temperature is reduced at higher molar masses of the grafting and ranges from 29.4 ± 0.1 °C for $X_n = 33$ to 24.9 ± 0.1 °C for $X_n = 538$ (Table 1 and Figure 2B "P*n*PrOx grafted"). While the grafting and geometry of the pore make a direct comparison to measurements in free aqueous solution

https://doi.org/10.1021/acs.nanolett.3c00438
Nano Lett. XXXX, XXX, XXX−XXX

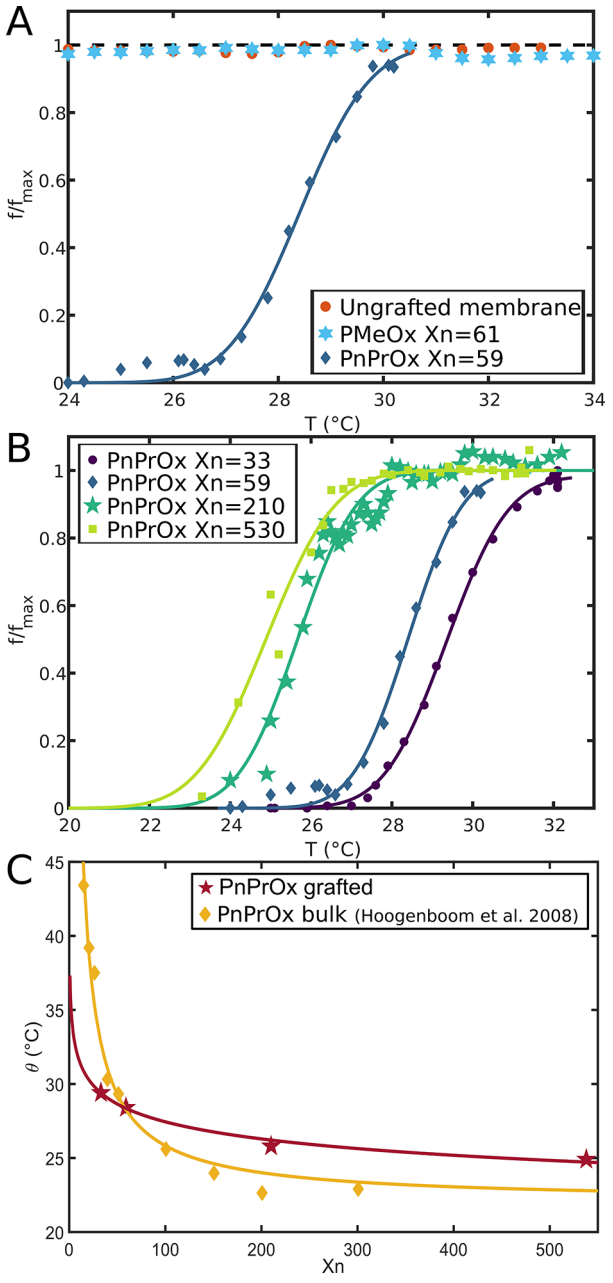

Figure 2. Normalized translocation frequency as a function of temperature for differently grafted pores. (A) Comparison of the frequency of translocation of λ-DNA as a function of temperature for PMeOx (X_n = 61), P*n*PrOx (X_n = 59), and ungrafted membrane. Pore diameter: 42 ± 0.5 nm. Applied pressure: 80 mbar. The blue solid line represents the fitting by the error function. The dashed black line represents the constant f/f_{max} = 1. Unaveraged curves are shown in section S8 in the Supporting Information. (B) Comparison of the frequency of translocation of λ-DNA as a function of temperature for different number-average degrees of polymerization of P*n*PrOx (X_n = 33, X_n = 59, X_n = 210, X_n = 538). Pore diameter: 42 ± 0.5 nm. Applied pressure: 80 mbar. Solid lines represent the fitting by error function. Unaveraged curves are shown in section S8 in the Supporting Information. (C) Transition temperature θ for different polymerization degrees X_n. Red stars correspond to the P*n*PrOx graftings used in this study. Yellow diamonds correspond to a study from Hoogenboom et al.[22] Solid lines represent model fitting with a power law $\theta = a \cdot X_n^b + \theta_\infty$. The exponent b is equal to −0.3 for our data and −0.9 for Hoogenboom et al.

challenging, the measured values are close (26 °C for the P*n*PrOx X_n = 33 and 23 °C for P*n*PrOx X_n = 59, measured using optical turbidity). For the PMeOx grafting and the membrane without polymer grafting, the translocation frequency was found to be temperature-independent (Figure 2A).

Interestingly, we find that the transition temperature θ systematically decreases with increasing chain length for P*n*PrOx (Figure 2C). A decrease in LCST with increasing chain length or degree of polymerization has been observed for several polymers.[22−25] We find that the transition temperatures for our grafted polymers are overall similar to values determined by Hoogenboom et al.[22] Ungrafted P*n*PrOx in aqueous solution show a less steep dependence on chain length (Figure 2C "PnPrOx bulk"). This difference in scaling behavior might be due to the effect of grafting the polymer onto a gold support, which has been shown previously to lead to an altered chain length dependence for PNIPAM.[24]

In another series of experiments (section S4 in the Supporting Information), we cooled the system until the translocation frequency reached zero. These results demonstrate the reversibility of the system and show that, at low temperature, the pore reaches a state that efficiently blocks DNA molecules.

Having established thermal gating by heating the entire device, we were also able to demonstrate an even simpler and more elegant alternative heating method: local heating using a fluorescence lamp (section S3 in the Supporting Information). We found that adsorption of heat from the light source by the membrane can indeed be used to locally control the transition between coil and globule and modulate transport through the pore.

A SIMPLE POLYMER MODEL CAN ACCOUNT FOR THE GATING EXPERIMENTS

To provide a deeper understanding of the polymer phase transition inside the nanopore, we compared the temperature gating observed in our experiments to a simple theoretical model. Our theoretical description of the gating phenomenon is based on the work of Halperin on grafted polymer chain collapse in poor solvent and the suction model[26,27] (see section S5 in the Supporting Information for more details). Briefly, the configuration of the grafted chains is modeled by a mean field theory. We assume that the free energy F of the chains is composed of two main contributions: F_{el} which accounts for the configurational entropy and F_{mix} which accounts for the interaction of the monomer units with the solvent and with the other monomer units. The total free energy can then be expressed as a function of the number of monomer units per chain N, the coil radius R, as well as v and w, the second and third virial coefficients which quantify the 2-monomer and 3-monomer interactions, respectively. The coil radius was then determined by the numerical minimization of the polymer chain free energy for each temperature. From this value, the effective radius of the pore R_{eff} and the critical pressure of translocation P_c are determined. Using the suction model, f the frequency of translocation as a function of temperature was finally calculated as

$$f = k\left(\frac{R_{eff}}{R_{pore}}\right)^4 \frac{P}{P_c^0} \exp\left(-\frac{P_c^0}{P}\left(\frac{R_{pore}}{R_{eff}}\right)^4\right)$$

https://doi.org/10.1021/acs.nanolett.3c00438
Nano Lett. XXXX, XXX, XXX−XXX

Table 1. Transition Temperature θ and Steepness m for Different Degrees of Polymerization of P*n*PrOx Grafting

	X_n			
	33	59	210	538
m (1/°C)	0.58 ± 0.03	0.66 ± 0.05	0.61 ± 0.05	0.52 ± 0.03
θ (°C)	29.4 ± 0.1	28.4 ± 0.2	25.8 ± 0.1	24.9 ± 0.1

with R_{pore} being the radius of the pore without polymer grafting and P_c^0 the critical pressure without polymer grafting (i.e for $R_{eff} = R_{pore}$).

The model predicts that the translocation frequency as a function of temperature exhibits a sharp transition between no translocation at low temperature and full transmission at high temperature (Figure 3A and see section S5 in the Supporting Information for details about the choice of parameters). The sharpness of the transition dominated by the influence of the third virial coefficient w may be varied by chemical modification of the polymer (change of side groups etc.). For w values, used here as a fitting parameter, between 10^{-3} and 10^{-4}, which is comparable to values from the literature,

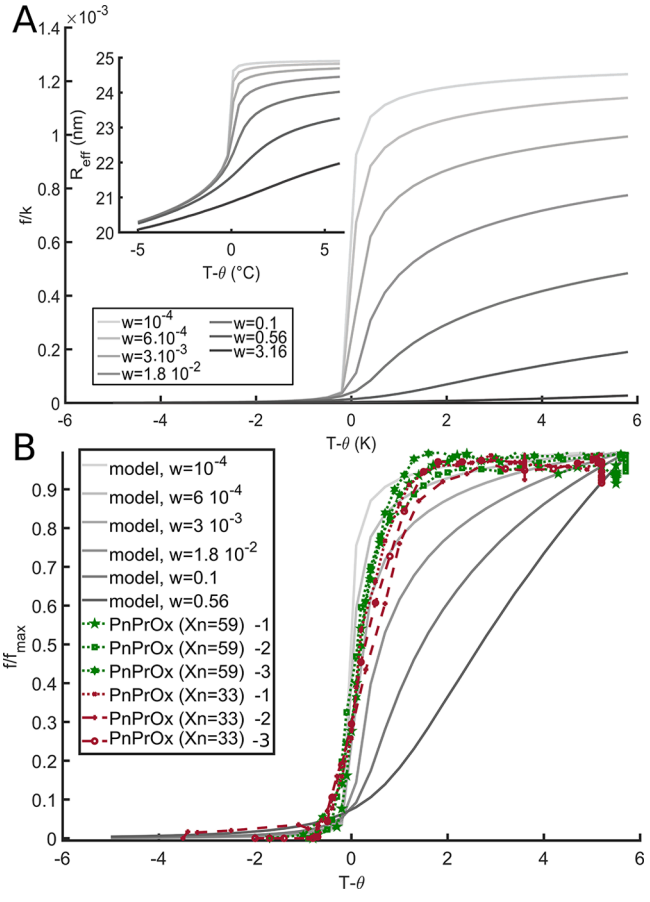

Figure 3. Theoretical modeling of the gating phenomenon. (A) (main) Modeling of the frequency of translocation normalized by the suction model prefactor k. This prefactor corresponds to the frequency of translocation for $P = P_c$. (inset) Modeling of the effective radius of the grafted nanopore, R_{eff}, as a function of temperature difference $T - \theta$ with θ being the critical temperature. Different values of the third virial coefficient w are represented by different colors. (B) Comparison between the coarse-grained model and individual translocation experiments (numbers 1−3) for different P*n*PrOx graftings (X_n = 33 and X_n = 59) normalized by the maximum frequency f_{max}.

this model reproduces well the transition observed experimentally for individual measurements with grafted polymers of different molar masses (Figure 3B).

This result shows that the key features of the temperature-induced gating can be readily recovered by a simple physical model including the collapse of the polymer inside the pore and the relation between the effective diameter of the pore and the energy barrier of the transport.

FLOW-DRIVEN DNA TRANSLOCATION EXPERIMENTS PROVIDE A TOOL TO CHARACTERIZE GRAFTED POLYMER LAYERS INSIDE NANOPORES

To examine the correlation between translocation frequency and the spatial extension of the polymer layer grafted inside the nanopore, we performed single-molecule ZMW experiments and measured the translocation frequency of DNA molecules through the membrane as a function of the applied pressure. Since the critical pressure of translocation depends strongly on pore radius $P_c \approx R_{pore}^{-4}$ (see section S6 in the Supporting Information), a small change in the pore radius is expected to result in a large difference in the critical pressure.

We recorded the frequency of translocation of DNA molecules for different graftings (PMeOx and P*n*PrOx) and degree of polymerization as a function of pressure (Figure 4A,B). Notably, the grafted polymers remained stable over a 6 month period (section S11 in the Supporting Information)

For the DNA translocation experiments using membranes with a PMeOx grafting, the experiments were performed at room temperature (20 °C), as the surrounding temperature had no influence on the translocation frequency for this grafting (Figure 2). For the experiments using membranes with a P*n*PrOx grafting of various polymerization degrees (X_n = 33, X_n = 59, X_n = 210, X_n = 538), we heated the system to a temperature higher than 30 °C. Heating the system made the grafted polymers collapse and, as a result, partially opened the pore (Figure 2). As a control experiment, we performed the same measurements with membranes with P*n*PrOx graftings at room temperature (20 °C). In the same pressure range, we recorded no translocation events, confirming the assumption that the pores were indeed closed at 20 °C.

All the pressure−frequency curves were fitted with the suction model,[27] and the results were then compared to the findings originating from membranes without a polymer grafting.[19] For the track-etched pores used here, the radius measured by electron microscopy (see section S9 in the Supporting Information), R_{pore} = 21 ± 0.25 nm, Auger et al. found the critical pressure to be P_c^0 = 82 ± 4 mbar in the absence of grafting polymers. We used these values to calculate the thickness of the grafted polymer layer. As shown in section S6 in the Supporting Information, the effective thickness of the polymer layer (R_p) can indeed be expressed as

$$R_p = R_{pore}(1 - (P_c^0/P_c)^{1/4})$$

https://doi.org/10.1021/acs.nanolett.3c00438
Nano Lett. XXXX, XXX, XXX−XXX

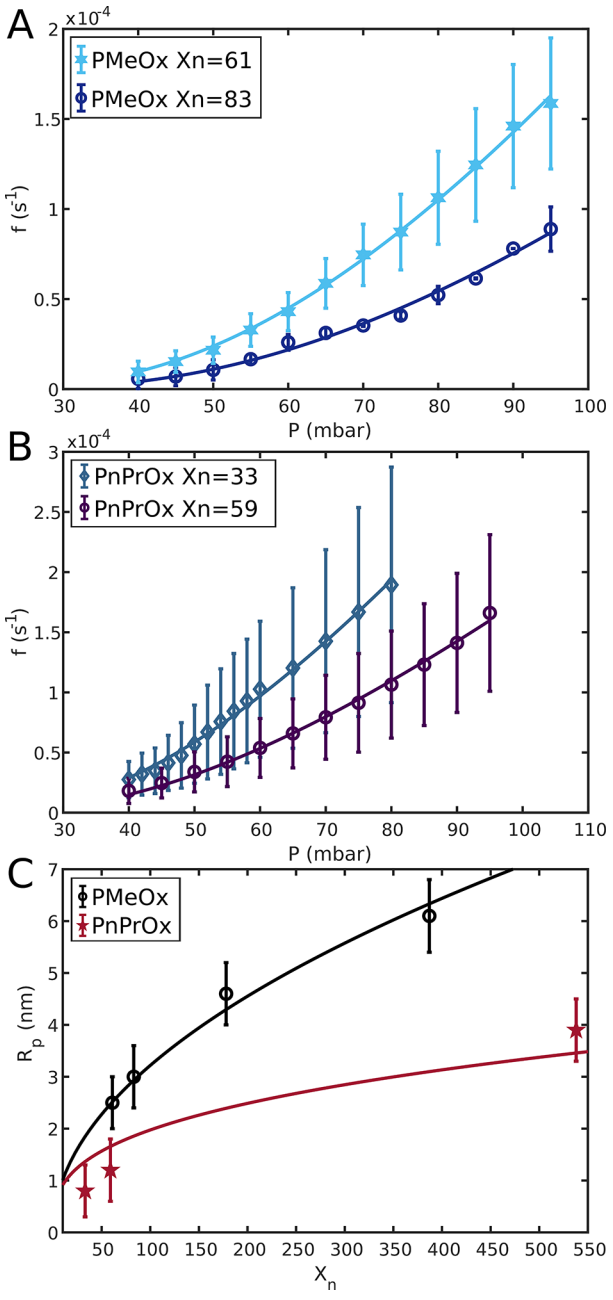

Figure 4. Averaged translocation frequency as a function of the applied pressure for different graftings. Frequency of translocation of λ-DNA was measured for membranes grafted with (A) PMeOx X_n = 61 in light blue and X_n = 83 in dark blue and (B) P*n*PrOx X_n = 33 in blue and X_n = 59 in purple at high temperature (T = 30 °C). Pore diameter: 42 ± 0.5 nm. The solid lines correspond to the suction model, which provides the critical pressure P_c as well as the constant k. The different polymers grafting inside the pore lead to a change in translocation frequency, implying a different state of openness of the nanopore that can be related to an effective radius of the pore. Each experiment was repeated at least 3 times. Error bars are standard errors. Unaveraged curves are shown in section S8 in the Supporting Information. (C) Evolution of the grafted polymer thickness R_p as a function of polymerization degree X_n for various graftings. Black circles represent PMeOx graftings, and red stars represent P*n*PrOx graftings. Solid lines correspond to a fit with a simple scaling law: $R_p = a \cdot X_n^{\nu}$ with ν = 0.5 for PMeOx and ν = 0.33 for P*n*PrOx. We found a(PMeOx) = 0.32 nm and a(P*n*PrOx) = 0.43 nm.

where P_c is the critical pressure for the pore grafted with polymers. This relation was checked with mPEG graftings by measuring the critical pressure P_c for different molecular masses of the grafted polymer (see section S6 in the Supporting Information).

The systematic variation in critical pressures with polymer type and length (Table 2) shows that the translocation of DNA through nanopores is strongly influenced by the grafting inside the pore. The observed trends are consistent with the additional polymer layer controlling the translocation by reducing the diameter of the nanopore. As a result, the DNA molecules to be transported must be spatially confined even further, and consequently, the critical pressure increases with increasing thickness of the polymer grafting.

For both PMeOx and P*n*PrOx, the increase of grafted polymer thickness R_p with polymerization degree X_n is well-described by power-law fits of the form $R_p = aX_n^{\nu}$ (Figure 4C). For PMeOx, we have used the scaling exponent ν = 0.5, as expected for the end-to-end distance of an ideal polymer chain. The fitted Kuhn length a = 0.32 nm for PMeOx is on the same order of the theoretical monomer length obtained from its chemical structure (0.428 nm). These findings suggest that grafted PMeOx behaves like a flexible polymer chain in a good solvent, similar to PMeOx in free solution. In contrast, while the grafted polymer thickness for P*n*PrOx above the critical temperature (Figure 4C) also increases with increasing chain length, the observed values are much smaller. In this case, we have used the scaling exponent ν = 0.33, as expected for the end-to-end distance of a collapsed polymer in a bad solvent. The fitted apparent monomer length a = 0.43 nm, which is as expected larger than that of PMeOx.

These results support not only the idea that the P*n*PrOx polymers exhibit a reversible coil−globule transition inside the pore when heated above the LCST but also that our nanopore methodology can be used as a precise tool to determine grafted polymer thickness in nanoporous membranes.

THERMOSWITCHABLE NANOPORES CONTROL THE TRANSLOCATION OF VIRAL PARTICLES

As an application of the gating behavior observed for DNA molecules, we extended our approach to gating viral capsids derived from Adeno-Associated Virus (AAV) as a model system. We translocated viral particles (with a diameter of 25 ± 3 nm[28]) through grafted membranes (PMeOx and P*n*PrOx) and measured the translocation frequency as a function of the temperature. In this case, the pore diameter was chosen to be 200 nm in order to avoid self-interaction between viral capsids. The switching phenomenon observed for DNA molecules was also observed for AAV for P*n*PrOx grafting, but not for PMeOx grafting (Figure 5 and section S10 in the Supporting Information). Remarkably, the critical temperature measured for viral particles (T_{crit} = 25.5 °C for P*n*PrOx X_n = 210) was very close to that observed for DNA molecules (T_{crit} = 25.8 °C for P*n*PrOx X_n = 210). This result strengthens the idea that the grafted polymers of P*n*PrOx undergo a global reorganization during the coil−globule transition and that the toggle switch phenomenon observed is not limited to one type of transported biomolecule but has far-reaching relevance for a wide range of biological and nonbiological systems.

In this study, we report a thermally switchable and reversible gate for the transport and filtration of macromolecules and viral particles. The properties of this nanogate are controlled by a network of electrografted polymers. We systematically

https://doi.org/10.1021/acs.nanolett.3c00438
Nano Lett. XXXX, XXX, XXX−XXX

Table 2. Critical Pressure and Grafted Polymer Thickness Extracted from Our Experimental Data[a]

	polymer type						
	PMeOx	PMeOx	PMeOx	PMeOx	P*n*PrOx	P*n*PrOx	P*n*PrOx
X_n	61	83	178	387	33	59	538
L_c (nm)	26	36	76	166	14	25	230
$P_{c,grafted}$ (mbar)	135 ± 3	150 ± 4	223 ± 4	327 ± 7	96 ± 4	104 ± 2	185 ± 4
R_p, polymer thickness (nm)	2.5 ± 0.5	3 ± 0.6	4.6 ± 0.6	6.1 ± 0.7	0.8 ± 0.5	1.2 ± 0.6	3.9 ± 0.6

[a]For the track-etched pores used here, the radius was measured by electron microscopy, (R_{pore} = 21 ± 0.25 nm), and Auger et al. found the critical pressure to be P_c = 82 ± 4 mbar in the absence of grafting polymers.[19] For P*n*PrOx graftings, the experiments were carried out at T (31 °C) > LCST. The contour length, L_c (i.e., maximum length of the molecule), is the number of monomers multiplied by their size (MeOx and P*n*PrOx monomers are about 428 pm).

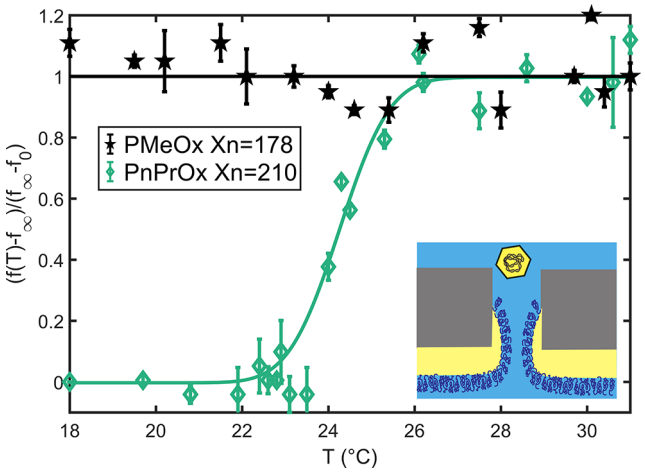

Figure 5. Controlled translocation of viral particles. Normalized frequency of translocation of AAV viral particles as a function of the temperature for two different graftings: black stars denote PMeOx and green diamonds denote P*n*PrOx. Pore diameter: 220 ± 1.8 nm. Applied pressure: 4 mbar. The green solid line is the result of fitting by an error function. The black solid line is the constant $(f(T) - f_\infty)/(f_\infty - f_0) = 1$. $N > 2$ for each experiment. Error bars are standard errors. Insert: scheme of an AAV virus at the entry of a grafted nanopore.

characterize the effects of the chemical composition and molar mass of the grafted macromolecules on the opening of the pore. In addition, we show that the transport properties of the membrane can be controlled by changes in temperature induced by light illumination via heating up the membrane.

The temperature switch between the extended and the collapsed state observed in this work for P*n*PrOx polymers occurs in a well-defined and sharp temperature range (~1 °C). Because of the limitation of our temperature measurement and averaging effects (see section S8 in the Supporting Information) we think that the steepness of this effective transition is in fact higher and may depend on the grafted polymer molar mass. The difference in transport properties between the two types of polymers at low temperature may be interpreted, beyond a simple coil−globule transition, as a difference in cohesivity of the network induced by the different chemical nature of the monomer units. A detailed investigation with polymers composed of a mixture of these two monomers might enable probing these effects in the future.

Future works may use this approach to investigate other viral capsid tolerance and plasticity and benefit from the proposed model to engineer the shape of the critical transition. Overall, we believe that nanopores grafted with thermoswitchable polymers have the potential to enable smart filters, act as sensors, and provide a new dimension of control over translocation, with possible applications in drinking water treatment, pharmaceutical production, and more.

■ ASSOCIATED CONTENT

Supporting Information

The Supporting Information is available free of charge at https://pubs.acs.org/doi/10.1021/acs.nanolett.3c00438.

Discussions, figures, and tables as described in the text (PDF)

Video recording of the translocation events (AVI)

■ AUTHOR INFORMATION

Corresponding Author

Fabien Montel − *Univ Lyon, ENS de Lyon, CNRS, Laboratoire de Physique, F-69342 Lyon, France;* orcid.org/0000-0001-5430-864X; Email: fabien.montel@ens-lyon.fr

Authors

Pauline J. Kolbeck − *Univ Lyon, ENS de Lyon, CNRS, Laboratoire de Physique, F-69342 Lyon, France; Department of Physics and Center for NanoScience, LMU Munich, 80799 Munich, Germany; Department of Physics and Debye Institute for Nanomaterials Science, Utrecht University, 3584 CC Utrecht, The Netherlands*

Dihia Benaoudia − *Université Paris Cité, ITODYS, CNRS, F-75006 Paris, France; Institut Parisien de Chimie Moléculaire, Equipe Chimie des Polymères, UMR CNRS 8232, Sorbonne Université, Paris 75252, France*

Léa Chazot-Franguiadakis − *Univ Lyon, ENS de Lyon, CNRS, Laboratoire de Physique, F-69342 Lyon, France*

Gwendoline Delecourt − *Institut Parisien de Chimie Moléculaire, Equipe Chimie des Polymères, UMR CNRS 8232, Sorbonne Université, Paris 75252, France*

Jérôme Mathé − *Université Paris-Saclay, Univ Evry, CNRS, LAMBE, 91000 Evry-Courcouronnes, France;* orcid.org/0000-0003-3883-3983

Sha Li − *Université Paris-Saclay, Univ Evry, CNRS, LAMBE, 91000 Evry-Courcouronnes, France*

Romeo Bonnet − *Université Paris Cité, ITODYS, CNRS, F-75006 Paris, France*

Pascal Martin − *Université Paris Cité, ITODYS, CNRS, F-75006 Paris, France;* orcid.org/0000-0003-1010-8421

Jan Lipfert − *Department of Physics and Center for NanoScience, LMU Munich, 80799 Munich, Germany; Department of Physics and Debye Institute for Nanomaterials Science, Utrecht University, 3584 CC Utrecht, The Netherlands;* orcid.org/0000-0003-3613-7896

https://doi.org/10.1021/acs.nanolett.3c00438
Nano Lett. XXXX, XXX, XXX−XXX

Anna Salvetti − *Centre International de Recherche en Infectiologie, INSERM U111, UMR CNRS 5308, Université Claude Bernard Lyon 1, Lyon 69007, France*

Mordjane Boukhet − *Center for Molecular Bioengineering (B CUBE), Technical University of Dresden, 01062 Dresden, Germany*

Véronique Bennevault − *Institut Parisien de Chimie Moléculaire, Equipe Chimie des Polymères, UMR CNRS 8232, Sorbonne Université, Paris 75252, France; University of Evry, Evry 91000, France*

Jean-Christophe Lacroix − *Université Paris Cité, ITODYS, CNRS, F-75006 Paris, France;* orcid.org/0000-0002-7024-4452

Philippe Guégan − *Institut Parisien de Chimie Moléculaire, Equipe Chimie des Polymères, UMR CNRS 8232, Sorbonne Université, Paris 75252, France;* orcid.org/0000-0002-4919-0779

Complete contact information is available at: https://pubs.acs.org/10.1021/acs.nanolett.3c00438

Author Contributions

▽P.J.K. and D.B. contributed equally to this work. F.M., P.G., J.-C.L., J.M., and S.L. conceived the project. D.B., R.B., P.M., and G.D. performed polymer synthesis, characterization, and electrografting on nanoporous membranes. A.S. produced the AAV capsids. P.J.K., L.C.-F., G.D., and M.B. performed nanopore experiments. P.J.K., L.C.-F., M.B., and F.M. performed data analysis. F.M. performed theoretical modeling. F.M., P.G., V.B., J.-C.L., J.M., and J.L. supervised the work. P.J.K., L.C.-F., and F.M. wrote the manuscript. All authors contributed to the ideas and reviewed the manuscript.

Notes

The authors declare no competing financial interest.

■ ACKNOWLEDGMENTS

The authors thank Jens Uwe-Sommer, Holger Merlitz, Cendrine Moskalenko, Martin Castelnovo, Saskia Brugère, Kassandra Gérard, Thomas Auger, Jean-Marc Di Meglio, Loic Auvray, Arthur Ermatov, Willem Vanderlinden, and Hermann Gaub for helpful comments and discussions. This work was supported by the Centre National de la Recherche Scientifique under the 80 Prime project "NanoViro" and the ANR "Golden Gates".

■ REFERENCES

(1) Caspi, Y.; Zbaida, D.; Cohen, H.; Elbaum, M. Synthetic Mimic of Selective Transport Through the Nuclear Pore Complex. *Nano Letters.* **2008**, *8* (11), 3728−34.

(2) Dekker, C. Solid-state nanopores. *Nature Nanotechnology.* **2007**, *2* (4), 209−15.

(3) Emilsson, G.; Sakiyama, Y.; Malekian, B.; Xiong, K.; Adali-Kaya, Z.; Lim, R. Y. H.; et al. Gating Protein Transport in Solid State Nanopores by Single Molecule Recognition. *ACS Cent Sci.* **2018**, *4* (8), 1007−14.

(4) Emilsson, G.; Xiong, K.; Sakiyama, Y.; Malekian, B.; Ahlberg Gagnér, V.; Schoch, R. L.; et al. Polymer brushes in solid-state nanopores form an impenetrable entropic barrier for proteins. *Nanoscale.* **2018**, *10* (10), 4663−9.

(5) Hriciga, A.; Lehn, J. M. pH regulation of divalent/monovalent Ca/K cation transport selectivity by a macrocyclic carrier molecule. *Proceedings of the National Academy of Sciences.* **1983**, *80* (20), 6426−8.

(6) Yameen, B.; Ali, M.; Neumann, R.; Ensinger, W.; Knoll, W.; Azzaroni, O. Ionic Transport Through Single Solid-State Nanopores Controlled with Thermally Nanoactuated Macromolecular Gates. *Small.* **2009**, *5* (11), 1287−91.

(7) Keyser, U. F.; Koeleman, B. N.; van Dorp, S.; Krapf, D.; Smeets, R. M. M.; Lemay, S. G.; et al. Direct force measurements on DNA in a solid-state nanopore. *Nature Physics.* **2006**, *2* (7), 473−7.

(8) Roman, J.; Français, O.; Jarroux, N.; Patriarche, G.; Pelta, J.; Bacri, L.; et al. Solid-State Nanopore Easy Chip Integration in a Cheap and Reusable Microfluidic Device for Ion Transport and Polymer Conformation Sensing. *ACS Sensors.* **2018**, *3* (10), 2129−37.

(9) Lepoitevin, M.; Ma, T.; Bechelany, M.; Janot, J.-M.; Balme, S. Functionalization of single solid state nanopores to mimic biological ion channels: A review. *Adv. Colloid Interface Sci.* **2017**, *250*, 195−213.

(10) Venkatesan, B. M.; Dorvel, B.; Yemenicioglu, S.; Watkins, N.; Petrov, I.; Bashir, R. Highly Sensitive, Mechanically Stable Nanopore Sensors for DNA Analysis. *Adv. Mater.* **2009**, *21* (27), 2771−6.

(11) Alem, H.; Duwez, A.-S.; Lussis, P.; Lipnik, P.; Jonas, A. M.; Demoustier-Champagne, S. Microstructure and thermo-responsive behavior of poly(N-isopropylacrylamide) brushes grafted in nanopores of track-etched membranes. *J. Membr. Sci.* **2008**, *308* (1), 75−86.

(12) Lokuge, I.; Wang, X.; Bohn, P. W. Temperature-Controlled Flow Switching in Nanocapillary Array Membranes Mediated by Poly(N-isopropylacrylamide) Polymer Brushes Grafted by Atom Transfer Radical Polymerization. *Langmuir.* **2007**, *23* (1), 305−11.

(13) Reber, N.; Küchel, A.; Spohr, R.; Wolf, A.; Yoshida, M. Transport properties of thermo-responsive ion track membranes. *J. Membr. Sci.* **2001**, *193* (1), 49−58.

(14) Reber, N.; Omichi, H.; Spohr, R.; Tamada, M.; Wolf, A.; Yoshida, M. Thermal switching of grafted single ion tracks. *Nuclear Instruments and Methods in Physics Research Section B: Beam Interactions with Materials and Atoms.* **1995**, *105* (1), 275−7.

(15) Spohr, R.; Reber, N.; Wolf, A.; Alder, G. M.; Ang, V.; Bashford, C. L.; et al. Thermal control of drug release by a responsive ion track membrane observed by radio tracer flow dialysis. *J. Controlled Release* **1998**, *50* (1), 1−11.

(16) Arroyo, N.; Balme, S.; Picaud, F. Impact of surface state on polyethylene glycol conformation confined inside a nanopore. *Journal of Chemical Physics.* **2021**, *154* (10), 104901.

(17) Chen, G.; Dormidontova, E. PEO-Grafted Gold Nanopore: Grafting Density, Chain Length, and Curvature Effects. *Macromolecules.* **2022**, *55* (12), 5222−32.

(18) Ma, T.; Arroyo, N.; Marc Janot, J.; Picaud, F.; Balme, S. Conformation of Polyethylene Glycol inside Confined Space: Simulation and Experimental Approaches. *Nanomaterials [Internet]* **2021**, *11* (1), 244.

(19) Auger, T.; Mathé, J.; Viasnoff, V.; Charron, G.; Di Meglio, J.-M.; Auvray, L.; et al. Zero-Mode Waveguide Detection of Flow-Driven DNA Translocation through Nanopores. *Phys. Rev. Lett.* **2014**, *113* (2), 028302.

(20) Lim, R. Y. H.; Deng, J. Interaction Forces and Reversible Collapse of a Polymer Brush-Gated Nanopore. *ACS Nano* **2009**, *3* (10), 2911−8.

(21) Caspi, Y.; Zbaida, D.; Cohen, H.; Elbaum, M. Anomalous Diffusion of High Molecular Weight Polyisopropylacrylamide in Nanopores. *Macromolecules.* **2009**, *42* (3), 760−7.

(22) Hoogenboom, R.; Thijs, H. M. L.; Jochems, M. J. H. C.; van Lankvelt, B. M.; Fijten, M. W. M.; Schubert, U. S. Tuning the LCST of poly(2-oxazoline)s by varying composition and molecular weight: alternatives to poly(N-isopropylacrylamide)? *Chemical Communications.* **2008**, No. 44, 5758−5760.

(23) Lessard, D. G.; Ousalem, M.; Zhu, X. X. Effect of the molecular weight on the lower critical solution temperature of poly(N,N-diethylacrylamide) in aqueous solutions. *Can. J. Chem.* **2001**, *79* (12), 1870−4.

(24) Shan, J.; Zhao, Y.; Granqvist, N.; Tenhu, H. Thermoresponsive Properties of N-Isopropylacrylamide Oligomer Brushes Grafted to Gold Nanoparticles: Effects of Molar Mass and Gold Core Size. *Macromolecules.* **2009**, *42* (7), 2696−701.

(25) Tong, Y. W.; Shoichet, M. S. Defining the Surface Chemistry of Ammonia-Modified Poly(tetrafluoroethylene-co-hexafluoropropylene) Films. *Macromolecules.* **1999**, *32* (10), 3464−8.
(26) Halperin, A. Collapse of grafted chains in poor solvents. *J. Phys. (Paris)* **1988**, *49* (3), 547−50.
(27) Gay, C.; de Gennes, P. G.; Raphaël, E.; Brochard-Wyart, F. Injection Threshold for a Statistically Branched Polymer inside a Nanopore. *Macromolecules.* **1996**, *29* (26), 8379−82.
(28) Mietzsch, M.; Barnes, C.; Hull, J. A.; Chipman, P.; Xie, J.; Bhattacharya, N.; et al. Comparative Analysis of the Capsid Structures of AAVrh.10, AAVrh.39, and AAV8. *Journal of Virology.* **2020**, *94* (6), No. e01769-19.

https://doi.org/10.1021/acs.nanolett.3c00438
Nano Lett. XXXX, XXX, XXX−XXX